STABILITY ANALYSIS FOR A MATHEMATICAL MODEL OF THE *lac* OPERON

By

JOSEPH M. MAHAFFY (*Dept. of Mathematical Sciences, San Diego State University, CA*)

AND

EMIL SIMEONOV SAVEV (*Dept. of Mathematical Sciences, San Diego State University, CA*)

Abstract. A mathematical model for induction of the *lac* operon is derived using biochemical kinetics and includes delays for transcription and translation. Local analysis of the unique equilibrium of this nonlinear model provides conditions for stability. Techniques are developed to determine Hopf bifurcations, and stability switching is found for the delayed system. Near a double bifurcation point a hysteresis of solutions to two stable periodic orbits is studied. Global analysis provides conditions on the model for asymptotic stability. The biological significance of our results is discussed.

1. Introduction. The classical example of positive feedback or *induction* of a bacterial gene is the *lac* operon for *Escherichia coli.* The biological theory for induction of a gene was developed by Jacob and Monod in the late 1950s. The first mathematical model for this process was developed by B. C. Goodwin [8]. Subsequently, several models for induction have been developed and analyzed [9, 12, 19, 21, 22]. These models use a single nonlinear production term for the mRNA of the induced gene, then have 1 to n additional linear differential equations representing the subsequent reactions that lead to the endproduct. The endproduct stimulates or induces the gene to produce more endproduct.

Griffith [9] uses Lyapunov functions to show that a three-dimensional induction model with only the origin as an equilibrium is globally asymptotically stable. Selgrade [21] extends Griffith's results and shows that when there are three equilibria, two equilibria are stable and the third equilibrium is a saddle with a two-dimensional stable manifold separating the domains of attraction of the other equilibria. For a four-dimensional extension of the Griffith model, Ji-Fa [12] uses Lyapunov functions to find sufficient conditions for stable equilibria. Selgrade [22] demonstrates that when this model is

extended to five dimensions, there exist parameters where a Hopf bifurcation occurs though these values clearly lie outside the range of biological significance.

With the *lac* gene of *E. coli* as an example, Mahaffy [16, 17] developed a mathematical model based more closely on this important biological case of induction. The *lac* operon is normally repressed by the binding of a repressor to the operator region of the *lac* gene. When *E. coli* has lactose as its primary source of carbon and energy, the repressor protein is inactivated by an isomer of lactose (allolactose). Allolactose is produced in the cell from lactose that is transported into the cell. This induces the *lac* gene to produce large quantities of the three enzymes β-galactosidase, β-galactoside permease, and β-thiogalactoside acetyl transferase. The permease transports lactose into the cell, where β-galactosidase breaks lactose into simple hexose sugars, glucose and galactose, that can be metabolized for energy. Figure 1.1 illustrates the primary reactions governed by the *lac* operon. For transcription to begin the *lac* gene also requires cAMP and CAP (catabolite gene activator protein). When the cell has glucose readily available, metabolism of lactose is suppressed. Glucose inhibits the permease and excludes the inducer from the cell. In addition, glucose acts as a catabolite repressor by affecting the levels of cAMP and indirectly repressing the *lac* operon. This saves the cell energy when a better source of carbon is available. More details of the biological processes can be found in Beckwith [3], Beckwith and Zipser [4], and Miller and Reznikoff [11].

Knorre [13] showed experimentally that when a culture of exponentially growing cells of *E. coli* is transferred from a glucose to a lactose medium, the activity of β-galactosidase oscillates with a period of approximately 50 minutes for about four oscillations. This result has inspired several mathematical models to explain the instabilities. Mahaffy [16, 17] analyzed a model for the *lac* operon that includes the coupling of induction and catabolite repression and a nonlinear degradation term. The study ignored the glucose inhibition and exclusion controls and concentrated on the instabilities that arose from the delayed negative feedback of catabolite repression. Analysis of the linearized model found critical delays when a Hopf bifurcation occurred, which resulted in stable periodic solutions about an equilibrium. A later experiment by Pih and Dhurjati [20] reversed the experiment of Knorre and had exponentially growing cells on a lactose medium shifted to a glucose medium where again oscillations were observed in the β-galactosidase activity. Their explanation suggests that the catabolite inhibition of the *lac* operon system regulates the protein activity and leads to oscillations in concurrence with the results of Mahaffy [17].

In this paper we examine the stability properties of a mathematical model based more closely on the biochemical processes of induction for the *lac* operon without the catabolite repression. We show that for some parameters there is global stability. For other cases we find the existence of Hopf bifurcations and stability switches. These analyses are presented below.

2. The model and local analysis. In this section we discuss a mathematical model for the *lac* operon, which is based on Fig. 1.1. A model examining only the induction process due to lactose is formulated using biochemical kinetics and several simplifying assumptions. A derivation of the model follows the steps outlined in Mahaffy [16]. The
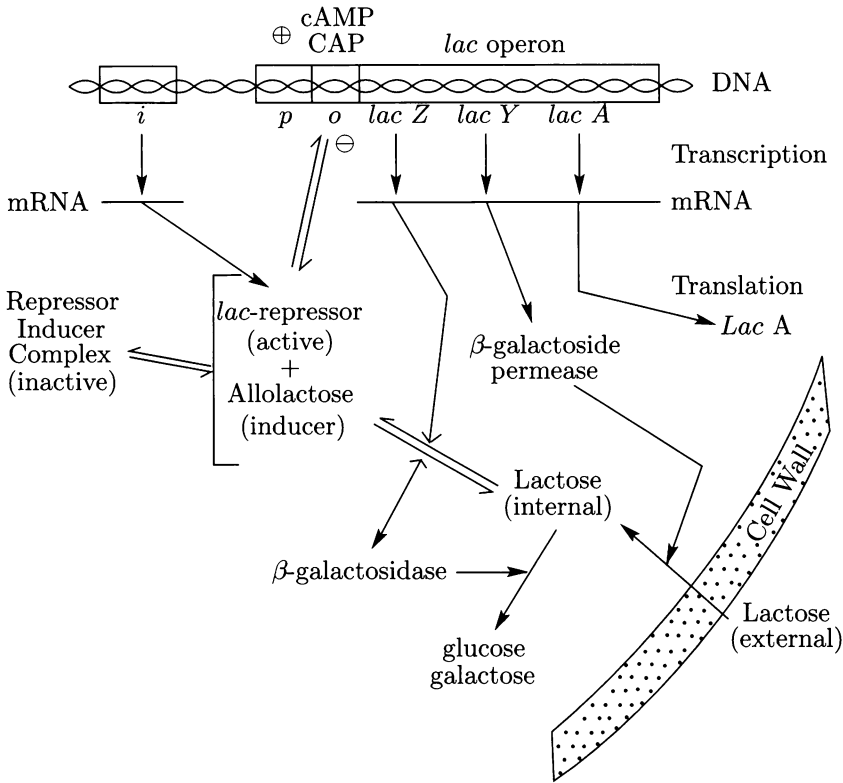
FIG. 1.1. Diagram of the *lac* operon showing the key biochemical reactions involved in induction

principal differences between the model studied here and the one developed before are the omission of catabolite repression and the inclusion of differing reaction rates for the production and degradation of β-galactoside permease and β-galactosidase.

The induction model examines the concentrations of the mRNA (y_1) transcribed from the *lac* gene, β-galactoside permease (y_2) and β-galactosidase (y_3) translated from the mRNA, and lactose (y_4) that is transported into the cell. After a rescaling of the variables, a reasonable mathematical model for the *lac* operon is given by the following system of four differential equations:

$$\dot{y}_1 = \frac{1 + k_1 y_4^\rho}{1 + y_4^\rho} - b_1 y_1,$$

$$\dot{y}_2 = y_1 - b_2 y_2, \qquad\qquad\qquad (2.1)$$

$$\dot{y}_3 = r_3 y_1 - b_3 y_3,$$

$$\dot{y}_4 = S y_2 - y_3 y_4.$$

With $k_1 > 1$, the first of these equations shows that the production of mRNA increases with increasing concentrations of the inducer, lactose, entering the cell, while mRNA is lost by a standard linear decay. The production of both enzymes depends linearly on the amount of mRNA, and they use standard linear decay (mostly through dilution

from growth of the cell). The concentration of the internal lactose (y_4) depends on the external concentration of lactose (S), which is assumed to be constant, and the concentration of the permease. The lactose is metabolized by β-galactosidase, which results in the nonlinear degradation term.

This model has many similarities to the induction models that have been studied previously [9, 12, 19, 21], but there are some significant differences. Most studies have examined equations of the form:

$$\dot{y}_1 = \frac{1 + k_1 y_n^\rho}{1 + y_n^\rho} - b_1 y_1,$$

$$\dot{y}_i = y_{i-1} - b_i y_i, \quad i = 2, \ldots, n. \tag{2.2}$$

Below our analysis compares and contrasts the model (2.1), which is based on the *lac* operon, to other induction models given by (2.2).

The expression of the *lac* operon requires transcription of the gene, then translation of the resultant mRNA to produce the enzymes, β-galactoside permease and β-galactosidase. These processes require a significant amount of time (about 30–60 sec.) as compared to the reaction times for the other biochemical species. Thus, it is appropriate to include time delays for transcription and translation. After rescaling, these delays are included as a single delay to create a system of delay differential equations that is the same as (2.1) except for the first equation,

$$\dot{y}_1(t) = \frac{1 + k_1 [y_4(t - \tau)]^\rho}{1 + [y_4(t - \tau)]^\rho} - b_1 y_1(t),$$

$$\dot{y}_2(t) = y_1(t) - b_2 y_2(t),$$

$$\dot{y}_3(t) = r_3 y_1(t) - b_3 y_3(t), \tag{2.3}$$

$$\dot{y}_4(t) = S y_2(t) - y_3(t) y_4(t).$$

Our analysis below examines the stability properties of both systems (2.1) and (2.3).

Our analysis begins by examining equilibria. The models of the form (2.2) have one to three equilibria depending on the values of the parameters, and thus exhibit a hysteresis as the parameters change. It has been argued that when there are three equilibria, the lower one represents basal levels of enzyme production, while the upper value is the induced state [9]. The middle equilibrium is a saddle node with its stable manifold being the separatrix between the other equilibria. However, this argument is not consistent with the biology of this problem since *E. coli* is either in an induced state or not depending on the environmental parameters, suggesting a unique equilibrium that is controlled by the external concentration of lactose. System (2.1) has a unique equilibrium point given

by the following:

$$\overline{y}_1 = \frac{b_2^\rho r_3^\rho + k_1 S^\rho b_3^\rho}{b_1(b_2^\rho r_3^\rho + S^\rho b_3^\rho)},$$

$$\overline{y}_2 = \frac{\overline{y}_1}{b_2} = \frac{b_2^\rho r_3^\rho + k_1 S^\rho b_3^\rho}{b_1 b_2(b_2^\rho r_3^\rho + S^\rho b_3^\rho)},$$

$$\overline{y}_3 = \frac{r_3 \overline{y}_1}{b_3} = \frac{r_3(b_2^\rho r_3^\rho + k_1 S^\rho b_3^\rho)}{b_1 b_3(b_2^\rho r_3^\rho + S^\rho b_3^\rho)},$$

$$\overline{y}_4 = \frac{b_3 S}{b_2 r_3}.$$

(2.4)

Note that the delayed system has the above constant functions for its equilibrium. It is easily seen that the equilibrium (2.4) increases as the concentration of external lactose (S) increases.

Studies of (2.2) show that when $n \leq 3$, there are no Hopf bifurcations. If a unique equilibrium exists, then it is a global attractor [9]. When there are three equilibria, then the state space separates into two domains of attraction with two attracting equilibria [21]. Selgrade [22] was only able to prove the existence of a Hopf bifurcation for the largest equilibrium for $n \geq 5$. Existence of periodic solutions for (2.2) with $n = 4$, the same dimension as (2.1), remains an open question though Ji-Fa [12] has proven a sufficient condition for stability.

To study the local stability, our model for the *lac* operon is linearized about its unique equilibrium. The linearization of (2.1) yields

$$\begin{pmatrix} \dot{y}_1 \\ \dot{y}_2 \\ \dot{y}_3 \\ \dot{y}_4 \end{pmatrix} = \begin{pmatrix} -b_1 & 0 & 0 & f'(\overline{y}_4) \\ 1 & -b_2 & 0 & 0 \\ r_3 & 0 & -b_3 & 0 \\ 0 & S & -\overline{y}_4 & -\overline{y}_3 \end{pmatrix} \begin{pmatrix} y_1 \\ y_2 \\ y_3 \\ y_4 \end{pmatrix},$$

(2.5)

where

$$f'(\overline{y}_4) = \frac{(k_1 - 1)\rho \overline{y}_4^{\rho-1}}{(1 + \overline{y}_4^\rho)^2} = \frac{(b_2 r_3)^{\rho+1}(k_1 - 1)\rho(S b_3)^{\rho-1}}{((b_2 r_3)^\rho + (S b_3)^\rho)^2}.$$

With $\overline{y}_4 = S b_3/(b_2 r_3)$, it can be shown that the characteristic equation for (2.5) is given by

$$(\lambda + b_1)(\lambda + b_2)(\lambda + b_3)(\lambda + \overline{y}_3) - \frac{f'(\overline{y}_4) S \lambda (b_2 - b_3)}{b_2} = 0.$$

(2.6)

A similar linearization about the equilibrium solution for the model of the *lac* operon with delays (2.3) yields its characteristic equation, which is an exponential polynomial given by the following:

$$(\lambda + b_1)(\lambda + b_2)(\lambda + b_3)(\lambda + \overline{y}_3) - \frac{e^{-\lambda \tau} f'(\overline{y}_4) S \lambda (b_2 - b_3)}{b_2} = 0.$$

(2.7)

3. Local stability and a Hopf bifurcation. The mathematical model given by (2.1) contains seven kinetic parameters (eight for (2.3) including the delay). Biologically, the kinetic decay rates, b_2 and b_3 should be approximately equal since β-galactoside permease and β-galactosidase are stable proteins. The primary decrease in concentration

of y_2 and y_3 is due to dilution caused by cell growth, i.e., b_2 and b_3 are approximately equal to $\ln(2)$ divided by the cell doubling time. For the biologically important case where $b_2 = b_3$, we have the following result:

THEOREM 3.1. *If $b_2 = b_3$, then the equilibrium of* (2.1) *or the delayed system* (2.3) *is locally stable.*

Proof. The proof of this result follows immediately. When $b_2 = b_3$, the characteristic equations (2.6) and (2.7) reduce to a factored polynomial with the four negative roots $-b_1, -b_2, -b_3$, and $-\overline{y}_3$. Thus, the equilibrium is locally asymptotically stable for either system.

Because of the continuous dependence of the eigenvalues from the characteristic equations (2.6) and (2.7), it follows from Theorem 3.1 that if b_2 is close to b_3, then the equilibrium of (2.1) or (2.3) is locally stable. However, as b_2 and b_3 separate with $b_2 > b_3$, then it is apparent that the last term on the left-hand side of (2.6) could become sufficiently negative that the sign of the λ coefficient becomes negative, which implies by the Routh-Hurwitz criteria [7] that at least one eigenvalue has positive real part and the equilibrium of (2.1) is locally unstable. Example 3.1 below illustrates this situation. As is often the case, the delayed system (2.3) is easier to destabilize.

The special case $\rho = 1$ allows the complete analysis of (2.6), which is summarized in the following theorem:

THEOREM 3.2. *If $\rho = 1$, then the equilibrium of* (2.1) *is locally stable.*

Proof. The characteristic equation (2.6) can be expanded to a fourth-degree polynomial, $\lambda^4 + a_1\lambda^3 + a_2\lambda^2 + a_3\lambda + a_4 = 0$, where

$$a_1 = b_1 + b_2 + b_3 + \overline{y}_3,$$

$$a_2 = b_1b_2 + b_1b_3 + b_1\overline{y}_3 + b_2b_3 + b_2\overline{y}_3 + b_3\overline{y}_3,$$

$$a_3 = b_1b_2b_3 + b_1b_2\overline{y}_3 + b_1b_3\overline{y}_3 + b_2b_3\overline{y}_3 - \frac{f'(\overline{y}_4)S(b_2 - b_3)}{b_2},$$

$$a_4 = b_1b_2b_3\overline{y}_3,$$

with $f'(\overline{y}_4) = (k_1-1)b_2^2r_3^2/(b_2r_3+Sb_3)^2$ and $\overline{y}_3 = r_3(b_2r_3+k_1Sb_3)/(b_1b_3(b_2r_3+Sb_3))$. The Routh-Hurwitz criterion [7] gives all roots of (2.6) in the left half-plane, if the following determinants are positive:

$$D_2 \equiv \begin{vmatrix} a_1 & a_3 \\ 1 & a_2 \end{vmatrix} > 0, \qquad D_3 \equiv \begin{vmatrix} a_1 & a_3 & 0 \\ 1 & a_2 & a_4 \\ 0 & a_1 & a_3 \end{vmatrix} > 0,$$

$$D_4 \equiv \begin{vmatrix} a_1 & a_3 & 0 & 0 \\ 1 & a_2 & a_4 & 0 \\ 0 & a_1 & a_3 & 0 \\ 0 & 1 & a_2 & a_4 \end{vmatrix} > 0.$$

Note $D_4 = a_4D_3$, and so it suffices to show that $D_2 > 0$ and $D_3 > 0$. The expansions of both D_2 and D_3 in MAPLE yield long expressions that have only positive terms after

finding a common denominator and using the simplify command. Thus, the equilibrium of (2.1) is locally asymptotically stable.

Before proceeding with our first example, we discuss the technique employed for finding a Hopf bifurcation for the delayed system (2.3). As the delay τ is varied with all other parameters fixed, the technique of Mahaffy [15] is used to determine the value of the critical delay where this Hopf bifurcation occurs. Define the following expressions:

$$P(\lambda) \equiv (\lambda + b_1)(\lambda + b_2)(\lambda + b_3)(\lambda + \overline{y}_3)$$

and

$$Q \equiv \frac{f'(\overline{y}_4)S(b_2 - b_3)}{b_2}.$$

With these expressions the characteristic equation (2.7) is written

$$P(\lambda) = Q\lambda e^{-\lambda\tau}. \tag{3.1}$$

For a Hopf bifurcation to exist, (3.1) must be satisfied for $\lambda = i\omega$ with ω real.

Our technique for determining the critical delay, τ_{cr}, is to first find ω such that the magnitudes of both sides of (3.1) agree. Then the argument of the right-hand side is aligned with the argument of the left-hand side by adjusting τ. For a Hopf bifurcation to exist, there must be an ω such that the magnitude and argument of both sides of (3.1) are equal. Note that $|P(i\omega)|$ is monotonically increasing in ω with $P(0) > 0$ and $|P(i\omega)| > |Q\omega|$ for large ω, since P is quartic in ω. Thus, it requires a careful choice of parameters to satisfy $|P(i\omega^*)| = |Q\omega^*|$ for some ω^*. If this condition is satisfied, a Hopf bifurcation occurs when

$$\arg(P(i\omega^*)) = \frac{\pi}{2}\operatorname{sgn}(Q) - \omega^*\tau_{\mathrm{cr}} + 2k\pi$$

or

$$\tau_{\mathrm{cr}}(k) = \frac{1}{\omega^*}\left(2k\pi + \frac{\pi}{2}\operatorname{sgn}(Q) - \Theta(\omega^*)\right), \quad k = 0, 1, \ldots,$$

where $\Theta(\omega^*) \equiv \arctan(\omega^*/b_1) + \arctan(\omega^*/b_2) + \arctan(\omega^*/b_3) + \arctan(\omega^*/\overline{y}_3)$ and $\operatorname{sgn}(Q) = Q/|Q|$.

Below we present a series of examples that show local instabilities of (2.1) and (2.3) with numerical simulations suggesting stable Hopf bifurcations. Bifurcation diagrams are provided to illustrate how changes in some parameters affect our model of the *lac* operon. Previous studies of repression models have shown that the parameter influencing stability most is ρ [1, 14, 18]. Yagil and Yagil [23] analyzed kinetic experiments for the inducer IPTG, which binds like allolactose to the *lac* repressor to form the inactive complex. They found that most strains of *E. coli* require two molecules of IPTG ($\rho = 2$) to create the inactive complex, but some strains only need one molecule of IPTG ($\rho = 1$). (The active *lac* repressor has both dimeric and tetrameric forms that bind to the promoter and suppress transcription, but apparently the inactive tetrameric form does not require the inducer bound to all four sites.) Below we present two examples where the model can become unstable with $\rho = 2$. Theorem 3.2 shows that when $\rho = 1$, our model without delays for the *lac* operon is always locally stable. The next section provides some global stability results for $\rho = 1$.
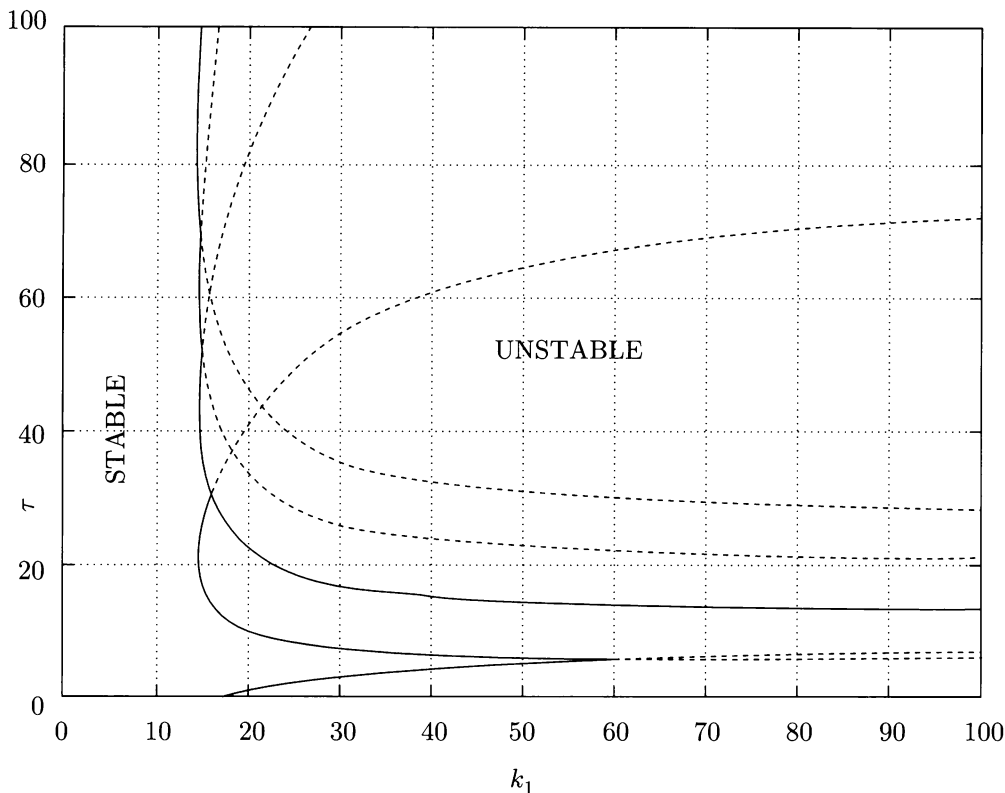
FIG. 3.1. Bifurcation curves for k_1 vs. τ. Solid lines show stability changes, while dashed lines give other purely imaginary eigenvalues.

EXAMPLE 3.1. Our first example considers a case when $b_2 > b_3$ ($b_2 = 2$ and $b_3 = 0.1$) and examines the behavior of the model (2.3) as the strength of induction k_1 and the delay τ are varied. The other parameters are fixed with $\rho = 2$, $b_1 = 1$, $r_3 = 0.1$, and $S = 1$. For each fixed $k_1 > 1$, (3.1) is used to compute which values of τ result in eigenvalues λ with purely imaginary part. Figure 3.1 shows the bifurcation curves for (2.3) in the (k_1, τ)-parameter space. Smaller values of k_1 ($k_1 < 14.8$) result in stability of (2.3) independent of the delay. The undelayed system (2.1) undergoes a supercritical Hopf bifurcation as k_1 increases through a critical value near 14.9. Numerical simulations of (2.1) for larger k_1 show stable limit cycles about the equilibrium.

A second phenomenon, which is readily apparent from the bifurcation diagram in Fig. 3.1, is the existence of stability switches for the system (2.3). The genetic control model of repression with delays was shown to have a single critical delay with a supercritical Hopf bifurcation to stable periodic orbits for all delays larger than the critical delay [18]. For this model of induction if we fix $k_1 = 17$, then it is clear that (2.1) is unstable. As the delay increases to 0.86, the System (2.3) becomes stable. When τ is further increased to 12.77, System (2.3) once again loses stability. For this value of k_1 there are no further stability switches, but Fig. 3.1 shows that for some k_1 values multiple stability switches

occur. Stability switches have been observed in other models with delays [5, 6] and represent an interesting property resulting from the infinite number of solutions to the characteristic equation (2.7).

Another result that is evident from Fig. 3.1 is the existence of double bifurcation points where two pairs of eigenvalues have purely imaginary parts. In our example, a double bifurcation point occurs at $k_1 = 74.71$ and $\tau = 6.301$ with eigenvalues $\lambda = \pm 0.09995i$ and $\pm 0.8346i$. Guckenheimer and Holmes [10] show that a variety of behaviors is possible near a double bifurcation point. In our model we observe a hysteresis between two stable limit cycles that depend on initial conditions in the region where two pairs of eigenvalues have positive real part.

Figure 3.2 shows a phase portrait in the (y_1, y_2, y_3)-phase space with two stable limit cycles for $k_1 = 120$ and $\tau = 6.3$ about the equilibrium point $(24.8, 12.4, 24.8, 0.5)^{\mathrm{T}}$. The larger orbit has a period of 65, while the smaller orbit has a period of 7.5. At $k_1 = 120$, there are a pair of eigenvalues $\lambda = \pm 0.873i$ when $\tau = 5.99$ and a pair of eigenvalues $\lambda = \pm 0.095i$ when $\tau = 6.97$. At $\tau = 6.3$, these pairs of eigenvalues each have positive real part ($\lambda = 0.0017 \pm 0.0995i$ and $\lambda = 0.0031 \pm 0.838i$), which yield two 2-dimensional attracting unstable manifolds each containing a stable periodic orbit. To numerically obtain both orbits we first found the smaller stable periodic orbit using $\tau = 6$, since its domain of attraction there is very large. The parameter τ was increased to 6.3 to obtain the solution pictured in Fig. 3.2. As τ is increased further to about 6.9, the domain of attraction for the unstable manifold of the large period orbit become sufficiently large that numerical simulations move to this stable periodic orbit. With these initial data the
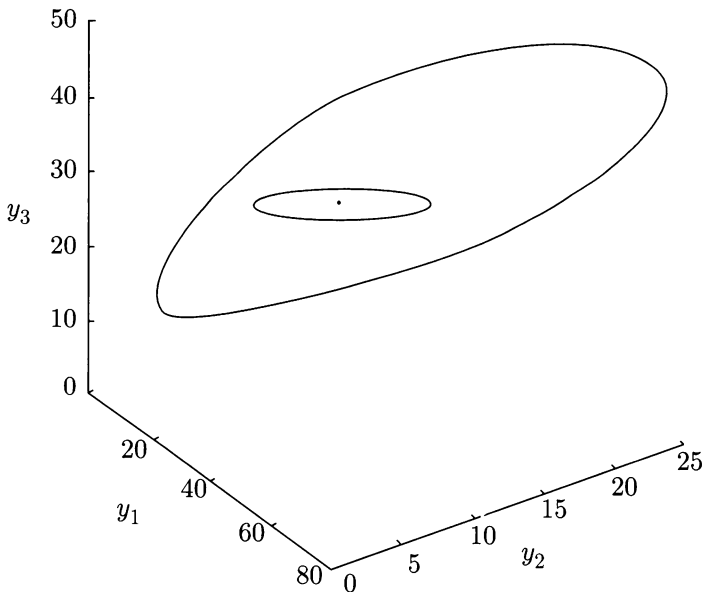

FIG. 3.2. Numerical simulation of (2.3) with $k_1 = 120$ and $\tau = 6.3$. The phase portrait shows the two stable periodic orbits possible in the (y_1, y_2, y_3)-phase space.
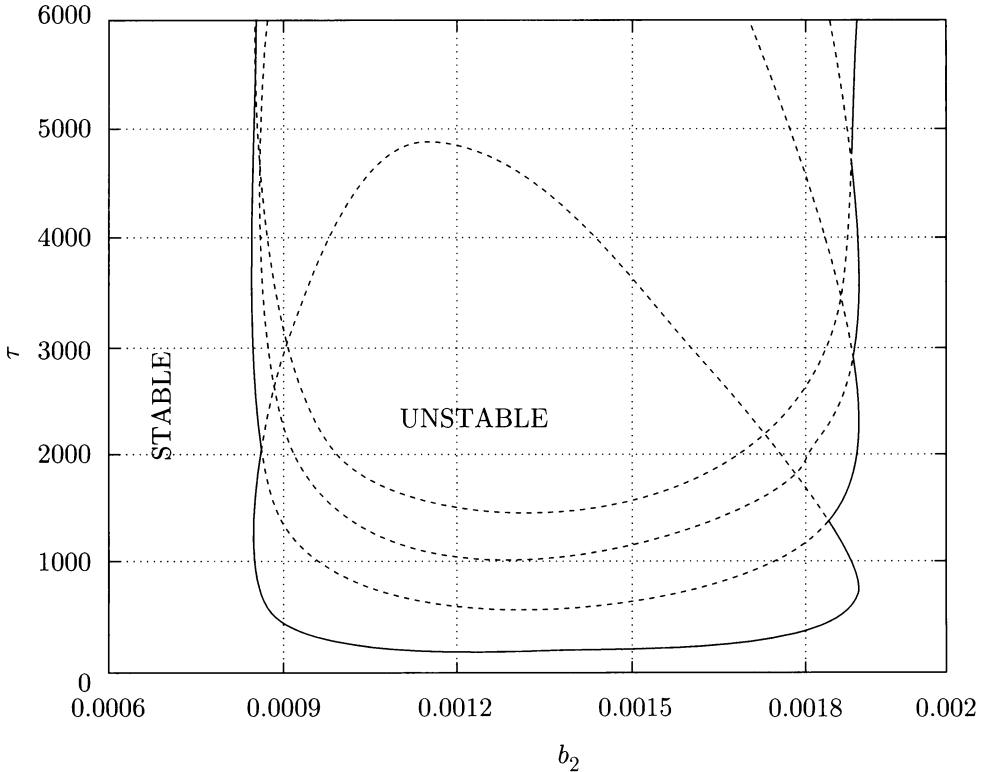
FIG. 3.3. Bifurcation curves for b_2 vs. τ. Solid lines show stability changes, while dashed lines give other purely imaginary eigenvalues.

delay is slowly decreased to 6.3 to obtain the other orbit seen in Fig. 3.2. The transitions between these two unstable manifolds give numerical simulations that are toroidal as one would expect. Thus, this example shows a hysteresis of solutions between two stable periodic orbits depending on initial data. Similar simulations have been produced for another delay differential equation by Bélair and Campbell [5].

EXAMPLE 3.2. When $b_3 > b_2$, all of the coefficients of the characteristic equations (2.6) and (2.7) are positive, which makes it more difficult to destabilize the systems of differential equations. This example studies the Hopf bifurcation curves for τ versus b_2 over an extremely limited range, $0.0006 < b_2 < 0.002$, while b_3 is fixed at 0.01. Figure 3.3 illustrates the bifurcation curves with the other parameters fixed at $k_1 = 10$, $b_1 = 10$, $r_3 = 1$, $S = 0.1$, and $\rho = 4$. The figure shows that very large delays are needed to destabilize this example.

In this example the undelayed system (2.1) is locally stable. In fact, the minimum delay that results in a Hopf bifurcation is $\tau = 150.33$ and $b_2 = 0.0013$. As in the previous example, the bifurcation diagram shows stability switches. For $\tau > 150.33$, our model (2.3) is stable for small b_2, then undergoes a supercritical Hopf bifurcation as b_2 increases, and finally restabilizes as b_2 increases further. For example, when $\tau = 1000$, System (2.3) is unstable for $0.0008542 < b_2 < 0.001875$. It is readily apparent from Fig. 3.3 that there

are some values of b_2 that result in stability switches as τ is increased, as occurred in the previous example.

EXAMPLE 3.3. As seen in Example 3.1, when $b_2 > b_3$, the nondelayed system (2.1) can be unstable for a value of ρ as low as 2. Example 3.2 had $b_2 < b_3$, but required large delays for a Hopf bifurcation. If $b_2 < b_3$, a much larger value of ρ is needed for the nondelayed system to become unstable. Consider the case $b_2 = 1$ and $b_3 = 10$. Fix the other parameters $k_1 = 10$, $b_1 = 1$, $r_3 = 1$, and $S = 0.1$. Analysis of the characteristic equation (2.6) using MAPLE showed that the lowest integer value of ρ that caused instabilities for (2.1) is 160. This is clearly outside the realm of biological interest, but it compares similarly to the results of Selgrade [22] who showed that (2.2) with $n = 5$ required $\rho \geq 205$ for a Hopf bifurcation.

4. Global analysis. The previous section provided a local analysis and numerical simulations demonstrating the existence of periodic solutions for our models of the *lac* operon. In this section we first establish that all positive solutions of (2.1) or (2.3) remain bounded and provide asymptotic bounds for these solutions. Next we prove for a range of the parameters that when the Hill coefficient $\rho = 1$, the solutions of (2.1) or (2.3) asymptotically approach the unique equilibrium. The arguments use differential inequalities, which do not depend on whether delays are present in the differential equations. However, the choice of the sequence of times, t_i^n, presented below does require consideration of the delay. Our techniques follow the work of Banks and Mahaffy [1, 2], which can be referenced for more details.

Let $\mathbf{R}_4^+$ be the positive orthant with ordered quadruples $[y_1, y_2, y_3, y_4]^{\mathrm{T}}$ and $y_i \geq 0$ for $i = 1, \ldots, 4$. From the system of differential equations (2.1) is is clear that $\mathbf{R}_4^+$ is invariant, i.e., all solutions of (2.1) with initial conditions in $\mathbf{R}_4^+$ remain in $\mathbf{R}_4^+$ for all $t \geq 0$. (Suppose $y_i(t) = 0$ at some t. Then $\dot{y}_i(t) \geq 0$. Hence, y_i is nondecreasing at t, and the solution cannot become negative.) This argument extends easily to the system of delay differential equations (2.3) with nonnegative initial data to show solutions remain nonnegative.

The positive feedback of induction implies that $k_1 > 1$. Since $y_4 \geq 0$, $f(y_4) \equiv (1 + k_1 y_4^\rho)/(1 + y_4^\rho)$ is bounded between 1 and k_1. In contrast to work on the repression model [1], which requires sequential establishment of upper then lower bounds, we establish lower and upper bounds simultaneously in the models for the *lac* operon to decrease some of the notational complications.

Our analysis begins by finding a lower bound and an upper bound for $y_1(t)$. Let $z_1^{l1}(0) = y_1(0) = z_1^{u1}(0)$ with $\dot{z}_1^{l1} = 1 - b_1 z_1^{l1}$ and $\dot{z}_1^{u1} = k_1 - b_1 z_1^{u1}$. Then $z_1^{l1}(t) \leq y_1(t) \leq z_1^{u1}(t)$ for all $t \geq 0$, since $\dot{z}_1^{l1}(t) \leq \dot{y}_1(t) \leq \dot{z}_1^{u1}(t)$. However,

$$z_1^{l1}(t) = \frac{1}{b_1} + \left(y_1(0) - \frac{1}{b_1}\right) e^{-b_1 t} \quad \text{and} \quad z_1^{u1}(t) = \frac{k_1}{b_1} + \left(y_1(0) - \frac{k_1}{b_1}\right) e^{-b_1 t}.$$

Thus given some $\varepsilon_1^1 > 0$ (sufficiently small), there exists $t_1^1 \geq 0$ such that both $z_1^{l1}(t) \geq \frac{1}{b_1} - \varepsilon_1^1 \equiv L_1^1$ and $z_1^{u1}(t) \leq \frac{k_1}{b_1} + \varepsilon_1^1 \equiv U_1^1$ for all $t \geq t_1^1$. Thus, $L_1^1 \leq y_1(t) \leq U_1^1$ for $t \geq t_1^1$.

A similar argument shows that for $z_2^{l1}(t_1^1) = y_2(t_1^1) = z_2^{u1}(t_1^1)$ and

$$\dot{z}_2^{l1} = \left(\frac{1}{b_1} - \varepsilon_1^1\right) - b_2 z_2^{l1} \quad \text{and} \quad \dot{z}_2^{u1} = \left(\frac{k_1}{b_1} + \varepsilon_1^1\right) - b_2 z_2^{u1},$$

there exist ε_2^1 and t_2^1, such that both $z_2^{l1}(t) \geq (1/(b_1 b_2)) - \varepsilon_2^1 \equiv L_2^1$ and $z_2^{u1}(t) \leq (k_1/(b_1 b_2)) + \varepsilon_2^1 \equiv U_2^1$ for $t \geq t_2^1$. Note that $\varepsilon_2^1 > \varepsilon_1^1/b_2$ and $t_2^1 \geq t_1^1$. Thus, $L_2^1 \leq y_2(t) \leq U_2^1$ for $t \geq t_2^1$.

The same method applied in parallel shows that if $z_3^{l1}(t_1^1) = y_3(t_1^1) = z_3^{u1}(t_1^1)$ and

$$\dot{z}_3^{l1} = r_3 \left(\frac{1}{b_1} - \varepsilon_1^1\right) - b_3 z_3^{l1} \quad \text{and} \quad \dot{z}_2^{u1} = r_3 \left(\frac{k_1}{b_1} + \varepsilon_1^1\right) - b_3 z_2^{u1},$$

then there exist ε_3^1 and t_3^1, such that both $z_3^{l1}(t) \geq (r_3/(b_1 b_3)) - \varepsilon_3^1 \equiv L_3^1$ and $z_3^{u1}(t) \leq (k_1 r_3/(b_1 b_3)) + \varepsilon_3^1 \equiv U_3^1$ for $t \geq t_3^1$. Note that $\varepsilon_3^1 > \varepsilon_1^1 r_3/b_3$ and $t_3^1 \geq t_1^1$. Thus, $L_3^1 \leq y_3(t) \leq U_3^1$ for $t \geq t_3^1$.

The differential equation for y_4 has a nonlinear decay, which makes analysis of this equation slightly different from the methods used in Banks and Mahaffy [1]. It is essential that a positive lower bound for y_3 exists for decay of y_4. The differential inequality for the lower bound of y_4 uses the lower bound of y_2 for production and the upper bound of y_3 for the decay rate. With a related change for finding an upper bound for y_4, the analysis continues in a similar manner. Let $t_m^1 = \max\{t_2^1, t_3^1\}$. If $z_4^{l1}(t_m^1) = y_4(t_m^1) = z_4^{u1}(t_m^1)$ and

$$\dot{z}_4^{l1} = S \left(\frac{1}{b_1 b_2} - \varepsilon_2^1\right) - \left(\frac{k_1 r_3}{b_1 b_3} + \varepsilon_3^1\right) z_4^{l1},$$

$$\dot{z}_4^{u1} = S \left(\frac{k_1}{b_1 b_2} + \varepsilon_2^1\right) - \left(\frac{r_3}{b_1 b_3} - \varepsilon_3^1\right) z_4^{u1},$$

then there exist ε_4^1 and t_4^1 such that both $z_4^{l1}(t) \geq (Sb_3/(k_1 b_2 r_3)) - \varepsilon_4^1 \equiv L_4^1$ and $z_4^{u1}(t) \leq (Sk_1 b_3/(b_2 r_3)) + \varepsilon_4^1 \equiv U_4^1$ for $t \geq t_4^1$. Again ε_4^1 must be taken sufficiently small and $t_4^1 \geq t_m^1$. Thus, $L_4^1 \leq y_4(t) \leq U_4^1$ for $t \geq t_4^1$.

Having established a set of upper and lower bounds for the solution of (2.1), we proceed to iterate and improve those bounds using the same techniques applied above. At the nth iteration we assume that we have $L_i^n \leq y_i(t) \leq U_i^n$ for $t \geq t_i^n$. From our procedure above and the monotonic properties of the nonlinear function we can find ε_1^{n+1} sufficiently small and t_1^{n+1} such that if $t \geq t_1^{n+1}$, then

$$L_1^{n+1} \equiv \frac{1}{b_1} \left(\frac{1 + k_1 (L_4^n)^\rho}{1 + (L_4^n)^\rho}\right) - \varepsilon_1^{n+1}$$

$$\leq y_1(t) \leq \frac{1}{b_1} \left(\frac{1 + k_1 (U_4^n)^\rho}{1 + (U_4^n)^\rho}\right) + \varepsilon_1^{n+1} \equiv U_1^{n+1}.$$

Similar arguments yield ε_i^{n+1} sufficiently small and t_i^{n+1} with $i = 2, 3, 4$ such that

$$L_2^{n+1} \equiv \frac{1}{b_2} L_1^{n+1} - \varepsilon_2^{n+1} \leq y_2(t) \leq \frac{1}{b_2} U_1^{n+1} + \varepsilon_2^{n+1} \equiv U_2^{n+1}, \quad t \geq t_2^{n+1},$$

$$L_3^{n+1} \equiv \frac{r_3}{b_3} L_1^{n+1} - \varepsilon_3^{n+1} \leq y_3(t) \leq \frac{r_3}{b_3} U_1^{n+1} + \varepsilon_3^{n+1} \equiv U_3^{n+1}, \quad t \geq t_3^{n+1},$$

$$L_4^{n+1} \equiv \frac{S L_2^{n+1}}{U_3^{n+1}} - \varepsilon_4^{n+1} \leq y_4(t) \leq \frac{S U_2^{n+1}}{L_3^{n+1}} + \varepsilon_4^{n+1} \equiv U_4^{n+1}, \quad t \geq t_4^{n+1}.$$

By taking the ε_i^n sufficiently small and converging to zero, we construct monotonic sequences $\{L_i^n\}$ and $\{U_i^n\}$. The former sequence is monotonically increasing and bounded above; so the sequence converges to a limit, i.e., $L_i^n \to L_i^*$. Similarly, the sequence of upper bounds for the solution is monotonically decreasing and bounded below; so it converges to a limit, say $U_i^n \to U_i^*$.

From the arguments above it can easily be seen that the limiting sequences satisfy the following equations:

$$
\begin{aligned}
L_1^* &= \frac{1}{b_1}\left(\frac{1 + k_1(L_4^*)^\rho}{1 + (L_4^*)^\rho}\right), & U_1^* &= \frac{1}{b_1}\left(\frac{1 + k_1(U_4^*)^\rho}{1 + (U_4^*)^\rho}\right), \\
L_2^* &= \frac{1}{b_2}L_1^*, & U_2^* &= \frac{1}{b_2}U_1^*, \\
L_3^* &= \frac{r_3}{b_3}L_1^*, & U_3^* &= \frac{r_3}{b_3}U_1^*, \\
L_4^* &= \frac{SL_2^*}{U_3^*}, & U_4^* &= \frac{SU_2^*}{L_3^*}.
\end{aligned}
\tag{4.1}
$$

These results can be summarized in the following theorem:

THEOREM 4.1. *All solutions of (2.1) and (2.3) are bounded. Furthermore, for any $\varepsilon > 0$ there exists a T sufficiently large such that solutions of (2.1) and (2.3) satisfy $L_i^* - \varepsilon < y_i(t) < U_i^* + \varepsilon$ for $t \geq T$, where L_i^* and U_i^* are given by (4.1).*

The lower limit L_4^* and the upper limit U_4^* for the bounds on the solution $y_4(t)$ can be solved in terms of L_1^* and U_1^*, yielding

$$
L_4^* = \frac{Sb_3L_1^*}{b_2r_3U_1^*} \quad \text{and} \quad U_4^* = \frac{Sb_3U_1^*}{b_2r_3L_1^*}.
$$

These are substituted into the equations for the lower and upper limiting equations bounding $y_1(t)$, which give

$$
L_1^* = \frac{1}{b_1}\left(\frac{(b_2r_3U_1^*)^\rho + k_1(Sb_3L_1^*)^\rho}{(b_2r_3U_1^*)^\rho + (Sb_3L_1^*)^\rho}\right)
\tag{4.2}
$$

and

$$
U_1^* = \frac{1}{b_1}\left(\frac{(b_2r_3L_1^*)^\rho + k_1(Sb_3U_1^*)^\rho}{(b_2r_3L_1^*)^\rho + (Sb_3U_1^*)^\rho}\right).
\tag{4.3}
$$

It is clear that one of the solutions to these equations is always the equilibrium solution. From the previous section it is clear that there must be other solutions for certain ranges of the parameters. Consider Example 3.1. Solving (4.2) and (4.3) yields a fifth-order polynomial in either L_1^* or U_1^* with three positive real solutions, 1.002, 24.8, and 120.0. (The other solutions are complex.) Thus, Theorem 4.1 shows that $1.002 < y_1 < 120.0$ for t sufficiently large. Numerical simulations (shown in Fig. 3.2) of the larger of the two periodic orbits gave a lowest value of $y_1 = 6.64$, and the maximum of the orbit had $y_1 = 57.1$, which shows that the estimates above are conservative. The other bounds in Example 3.1 are found from (4.1) with $0.501 < y_2 < 60.0$, $1.002 < y_3 < 120.0$, and $0.004 < y_4 < 59.8$, which are again conservative estimates when compared to numerical values found for either of the two stable periodic orbits.

The bounds in Theorem 4.1 provide a global asymptotic stability result whenever it can be shown that $L_i^* = U_i^*$. The following corollary summarizes our stability result:

COROLLARY 4.1. *If the equilibrium $\bar{y}_1$ is the lowest $(L_1^* = \bar{y}_1)$, highest $(U_1^* = \bar{y}_1)$, or only positive solution to (4.2) and (4.3), then all positive solutions of (2.1) and (2.3) asymptotically approach the unique equilibrium solution.*

Proof. Suppose that the lowest positive solution of (4.2) and (4.3) is $L_1^* = \bar{y}_1$. Then by our arguments above, the sequence of lower bounds for the solution $y_1(t)$ converges to L_1^*. However, the upper bounds for $y_1(t)$ are linked to the lower bounds by (4.1). It is easily shown that the only solution for U_1^* of (4.2) and (4.3) with $L_i^* = \bar{y}_1$ is $U_i^* = \bar{y}_1$. Thus, $L_1^* = \bar{y}_1 = U_1^*$, and Theorem 4.1 gives the global asymptotic stability of the solutions of (2.1) and (2.3).

Banks and Mahaffy [1] showed that a repression model (similar to (2.2)) with $\rho = 1$ was globally asymptotically stable. In Section 3, we showed that (2.1) with $\rho = 1$ is locally stable. Furthermore, numerical studies of (2.1) and (2.3) with $\rho = 1$ indicate that all positive solutions approach the equilibrium. Below we present conditions that guarantee global asymptotic stability of the system of equations (2.1) or (2.3).

When $\rho = 1$, (4.2) and (4.3) can be solved simultaneously to give a cubic equation in L_1^* (or U_1^*). One solution is $\bar{y}_1$, while the other two solutions are given by

$$x_1 = \frac{A}{2} - \frac{1}{2}\sqrt{A^2 - \frac{4A\beta}{\beta - \sigma}} \quad \text{and} \quad x_2 = \frac{A}{2} + \frac{1}{2}\sqrt{A^2 - \frac{4A\beta}{\beta - \sigma}}, \tag{4.4}$$

where $\beta \equiv b_2 r_3$, $\sigma \equiv Sb_3$, and $A \equiv (k_1\sigma - \beta)/\sigma$. Since there are only three, we can apply Corollary 4.1 to obtain global stability of (2.1) or (2.3) unless $0 < x_1 < \bar{y}_1 < x_2$, where x_1 and x_2 satisfy (4.4).

PROPOSITION 4.1. *If $\rho = 1$ and $b_2 r_3 < Sb_3$, then all positive solutions of (2.1) or (2.3) approach the unique equilibrium solution.*

Proof. Since $b_2 r_3 < Sb_3$, it follows that $b_2 r_3 < k_1 Sb_3$ as $k_1 > 1$. Thus, $\beta - \sigma < 0$ and $k_1\sigma - \beta > 0$. This gives $4A\beta/(\beta - \sigma) < 0$. It follows that $x_1 < 0$, which implies that $\bar{y}_1$ is either the lowest or highest positive solution of (4.2) and (4.3). Corollary 4.1 completes the proof.

PROPOSITION 4.2. *If $\rho = 1$ and $b_2 r_3 > k_1 Sb_3$, then all positive solutions of (2.1) or (2.3) approach the unique equilibrium solution.*

Proof. Since $b_2 r_3 > k_1 Sb_3$, it follows that $b_2 r_3 > Sb_3$. Thus, $4A\beta/(\beta - \sigma) < 0$. The remainder of the proof follows the previous proposition.

Propositions 4.1 and 4.2 provide easy conditions to test for global stability of the unique equilibrium when $\rho = 1$. It remains to examine what happens when $b_2 r_3 - k_1 Sb_3 < 0 < b_2 r_3 - Sb_3$. It is easily seen in this case that (4.4) gives $x_1 > 0$. Note that the discriminant in (4.4) can be written

$$\Delta \equiv \frac{(\beta - k_1\sigma)(\beta^2 + (3 - k_1)\beta\sigma + k_1\sigma^2)}{\sigma^2(\beta - \sigma)}.$$

When $\Delta = 0$, it follows that $\beta^2 + (3 - k_1)\beta\sigma + k_1\sigma^2 = 0$. A simple calculation shows $\overline{y}_1 = A/2$; so $x_1 = \overline{y}_1 = x_2$, and again the equilibrium solution of (2.1) and (2.3) is globally asymptotically stable.

Our final stability result requires one of the following hypotheses:

(H1) $1 < k_1 \leq 9$,

(H2) $\frac{b_2 r_3}{Sb_3} \leq \frac{1}{2}(k_1 - 3 - \sqrt{k_1^2 - 10k_1 + 9})$ and $k_1 > 9$.

(H3) $\frac{b_2 r_3}{Sb_3} \geq \frac{1}{2}(k_1 - 3 + \sqrt{k_1^2 - 10k_1 + 9})$ and $k_1 > 9$.

In (H2) and (H3) we need $k_1 > 9$ to avoid complex solutions on the right-hand side of the first inequality.

THEOREM 4.2. *Let $\rho = 1$ and suppose that $b_2 r_3 - k_1 Sb_3 < 0 < b_2 r_3 - Sb_3$ with one of (H1), (H2), or (H3) being satisfied. Then all positive solutions of (2.1) or (2.3) approach the unique equilibrium solution.*

Proof. Note that when $\beta - k_1\sigma < 0 < \beta - \sigma$ and $\Delta > 0$, computations using MAPLE show that $0 < x_1 < \overline{y}_1 < x_2$, which fails to produce a stability result. However, if $\Delta \leq 0$ with $\rho = 1$, then $\overline{y}_1$ is the only real solution of (4.2) and (4.3). The stability of the equilibrium follows immediately.

For $\beta - k_1\sigma < 0 < \beta - \sigma$ and $\Delta \leq 0$, we must have $\beta^2 + (3 - k_1)\beta\sigma + k_1\sigma^2 \geq 0$. However, by examining this inequality as a quadratic function in β/σ, we see that the inequality holds whenever one of (H1), (H2), or (H3) is satisfied. This completes the proof of the theorem.

5. Discussion. The *lac* operon is a classical example of induction in *E. coli* with many experimental studies having been performed. Several earlier models of induction [8, 9, 19, 21] fail to account for the specific biochemical kinetics of the *lac* operon. This study examines the mathematical properties of a model derived from the induction process for the *lac* operon, ignoring catabolite repression and the enzymatic inhibition of β-galactoside permease by glucose, an endproduct of lactose catabolism. Our model is a system of four delay differential equations, (2.3), that represent the intracellular concentrations of the key elements in the induction of the *lac* operon and the catabolism of lactose.

Since experimental studies have shown oscillations in the intracellular concentration of β-galactosidase [13, 20], our theoretical studies examined the possibility that the induction process is the cause of these instabilities. Our model has a unique equilibrium solution about which we performed a local analysis. When the decay rates of the enzymes β-galactoside permease and β-galactosidase are the same, our model is locally stable. We showed that when the Hill coefficient $\rho = 1$, the system of equations without the delay (2.1) is locally asymptotically stable. For higher values of ρ, Hopf bifurcations can occur, and the system becomes unstable. Several examples illustrate the interesting bifurcation properties for this particular model. We demonstrated the existence of double bifurcation points that separated from a stable equilibrium into two distinct 2-D unstable manifolds each containing a stable periodic orbit. The preferred stable orbit, each with its own distinct period and amplitude depending from which pair of eigenvalues it

evolved, depended on the initial data. We also showed that this model allows multiple stability switches as one of the parameters is varied.

Differential inequalities were used to show that all positive solutions eventually enter a bounded invariant region. Under certain conditions on the parameters this region collapses to the unique equilibrium solution, which gives global asymptotic stability of (2.3) independent of the delay. In the case $\rho = 1$, very specific conditions on the parameters are presented to guarantee asymptotic stability of the equilibrium.

Our model for the *lac* operon produces several interesting mathematical results as noted above. We focused on the genetic control by induction to determine whether this positive feedback could explain the observed oscillations in several experiments. Our results suggest that experimental oscillations are not caused by the induction process. One key to producing bifurcations is a disparity between the parameters b_2 and b_3. However, these are the decay rates of the stable enzymes β-galactoside permease and β-galactosidase, which imply that b_2 and b_3 are nearly equal. When we produce periodic solutions in the model with delays, the period of the stable orbit is too short as compared to experimental oscillations. The experimental oscillations are approximately the same length as the cell doubling time, which is over 25 times greater than the combined delays for transcription and translation, while our model produces oscillations around 4–10 times the length of the delay. Finally, if we assume that one or two molecules of allolactose combine with the repressor molecule to prevent it from binding the *lac* operon, then ρ is small. We have shown that small values of ρ yield a very stable model.

In conclusion, our mathematical model supports the claim of Pih and Dhurjati [20] that the observed oscillations are probably not caused by the induction process. Instead, oscillations in β-galactosidase activity are likely the result of either some cell cycle event or catabolite repression. Thus, our mathematical model of the *lac* operon in *E. coli* supports the biological claim that other cellular controls are responsible for the experimental oscillations. Our analysis indicates that further modeling efforts could aid biologists in understanding the key controlling events for certain biochemical processes in procaryotic cells.

References

[1] H. T. Banks and J. M. Mahaffy, *Global asymptotic stability of certain models for protein synthesis and repression*, Quart. Appl. Math. **36**, 209–211 (1978)

[2] H. T. Banks and J. M. Mahaffy, *Stability of cyclic gene models for systems involving repression*, J. Theor. Biol. **74**, 323–334 (1978)

[3] J. R. Beckwith, *The lactose operon*. In F. Neidhardt, editor, *Escherichia coli and Salmonella typhimurium cellular and molecular biology*, volume 2, ASM, Washington, D.C., 1987, pp. 1444–1452

[4] J. R. Beckwith and D. Zipser, *The Lactose Operon*, Cold Spring Harbor Laboratory, Cold Spring Harbor, N.Y., 1970

[5] J. Bélair and S. A. Campbell, *Stability and bifurcations of equilibria in a multiple-delayed differential equation*, SIAM J. Appl. Math. **54**, 1402–1424 (1994)

[6] K. L. Cooke and Z. Grossman, *Discrete delay, distributed delay and stability switches*, J. Math. Anal. Appl. **86**, 592–627 (1982)

[7] F. R. Gantmacher, *The Theory of Matrices*, volume II, Chelsea, New York, 1959

[8] B. C. Goodwin, *Temporal Organization in Cells*, Academic Press, New York, 1963

[9] J. S. Griffith, *Mathematics of cellular control processes*, I; II, J. Theor. Biol. **20**, 202–208 (1968)

[10] J. Guckenheimer and P. Holmes, *Nonlinear Oscillations, Dynamical Systems and Bifurcations of Vector Fields*, Springer-Verlag, New York, revised edition, 1983

[11] J. H. Miller and W. S. Reznikoff, editors, *The Operon*, Cold Spring Harbor Laboratory, Cold Spring Harbor, N.Y., 1978

[12] J. Ji-Fa, *A Liapunov function for four-dimensional positive-feedback systems*, Quart. Appl. Math. **52**, 601–614 (1994)

[13] W. A. Knorre, *Oscillations of the rate of synthesis of β-galactosidase in Escherichia coli ML30 and ML308*, Biochem. Biophys. Res. Com. **31**, 812–817 (1968)

[14] J. M. Mahaffy, *Periodic solutions for certain protein synthesis models*, J. Math. Anal. Appl. **74**, 72–105 (1980)

[15] J. M. Mahaffy, *A test for stability of linear differential delay equations*, Quart. Appl. Math. **40**, 193–202 (1982)

[16] J. M. Mahaffy, *Cellular control models with linked positive and negative feedback and delays*, I. *The models*, J. Theor. Biol. **106**, 89–102 (1984)

[17] J. M. Mahaffy, *Cellular control models with linked positive and negative feedback and delays*, II. *Linear analysis and local stability*, J. Theor. Biol. **106**, 103–118 (1984)

[18] J. M. Mahaffy, *Stability of periodic solutions for a model of genetic repression with delays*, J. Math. Biol. **22**, 137–144 (1985)

[19] H. G. Othmer, *The qualitative dynamics of a class of biochemical control circuits*, J. Math. Biol. **3**, 53–78 (1976)

[20] N. P. Pih and P. Dhurjati, *Oscillatory behavior of β-galactosidase enzyme activity in Escherichia coli during perturbed batch experiments*, Biotech. Bioeng. **29**, 292–296 (1987)

[21] J. F. Selgrade, *Mathematical analysis of a cellular control process with positive feedback*, SIAM J. Appl. Math. **36**, 219–229 (1979)

[22] J. F. Selgrade, *A Hopf bifurcation in single-loop positive-feedback systems*, Quart. Appl. Math. **40** 347–351 (1982)

[23] G. Yagil and F. Yagil, *On the relation between effector concentration and the rate of induced enzyme synthesis*, Biophysical J. **11**, 11–27 (1971)